JOURNAL OF Materials CHEMISTRY

Liquid crystals based on pseudohalogold(I) isocyanide complexes

Mohamed Benouazzane, Silverio Coco, Pablo Espinet* and José M. Martín-Alvarez

Departamento de Química Inorgánica, Facultad de Ciencias, Universidad de Valladolid, E-47005 Valladolid, Spain. E-mail: espinet@qi.uva.es

Received 21st May 1999, Accepted 28th July 1999

Rod-like complexes [AuX(C≡NR)] (X = CN, SCN; R = $C_6H_4OC_nH_{2n+1}$-*p*, $C_6H_4C_6H_4OC_nH_{2n+1}$-*p* (*n* = 4, 6, 8, 10, 12); 2-F-4-$OC_{12}H_{25}C_6H_3$; 3-F-4-$OC_{12}H_{25}C_6H_3$; and 3,4,5-$(OC_{10}H_{21})_3C_6H_2$) have been prepared by reaction of [AuCl(C≡NR)] with KSCN or AgCN. The free phenyl isocyanides are not liquid crystals, but all the gold complexes display wide ranges of smectic A (S_A) mesophases, except the compound [Au(SCN)($CNC_6H_4OC_4H_9$)] which is not liquid crystalline, and the trialkoxyphenyl derivatives which show columnar hexagonal phases at room temperature. The determining influence of the electronic and structural characteristics of both the pseudohalo and isocyanide ligands on the stabilization and type of mesophase is discussed.

Introduction

Liquid crystals containing transition metals (metallomesogens) are already recognized as a distinct and interesting class of mesogens.[1–5]

Thermotropic mesomorphism is connected to the self-organization of individual molecules, which is a consequence of their shape, aspect ratio, and polar properties. The influence of these features in the appearance of mesophases is quite well understood for organic molecules, which have been studied for a long time. Therefore, it is interesting to advance similarly in the understanding of metallomesogens.

Although many transition metals and different ligands have been used to prepare liquid crystals we have chosen as a case study gold(I) complexes, which show a very simple coordination geometry and allow easier recognition of the influence of structural variations on the thermotropic behaviour.[6–13]

Recently, we have reported a family of mesomorphic gold(I) isocyanide complexes [Au(X)(C≡N$C_6H_4OC_nH_{2n+1}$)] (X = halogen, *n* = 2, 4, 6, 8, 10, 12) and, in order to understand the structure–properties relationship, we have studied the effects of both the isocyanide substituents and the anionic ligands on the mesogenic properties.[9–12] A comparison of these series allowed us to establish certain useful relationships between the molecular features of the complexes and their thermal behaviour.

In a continuation of this study, we look now at the effect of substituting halides for CN or SCN. This exchange is usually easy in most metal complexes and can provide a further way of tuning the thermotropic properties.

Results and discussion

Synthesis and characterization of the complexes

The syntheses of the gold(I) compounds were easily carried out from [AuCl(tht)] (tht = tetrahydrothiophene) by metathesis with the appropriate potassium or silver salts in acetone or dichloromethane according to Scheme 1.

All the complexes gave satisfactory C, H, N analyses which, together with yields and relevant IR data, are given in the experimental section.

The IR spectra of the cyanide complexes in dichloromethane solution show only one ν_{CN} absorption from the isocyanide group, in each case at higher wavenumbers (*ca.* 100 cm^{-1}) than for the corresponding free isocyanide, as expected.[9,10] In addition one ν_{CN} band appears at *ca.* 2160 cm^{-1} from the cyanide ligand, as has been reported for similar phosphine and isocyanide complexes.[14–16] In Nujol mulls the IR spectra are similar but the complexes [AuCN($CNC_6H_4OC_nH_{2n+1}$)] (*n* = 4, 6, 8, 10, 12) show a splitting of the ν_{CN} isocyanide band, possibly due to solid state effects.[17]

The thiocyanate ligand can bind Au(I) by the sulfur (Au-SCN) or the nitrogen (Au-NCS) atom giving rise to a pair of linkage isomers which can be characterized by IR spectroscopy.[18–21] The IR spectra in dichloromethane solution of the thiocyanate derivatives show one ν_{CN} band from the isocyanide group at about 2224 cm^{-1} and two ν_{CN} absorptions from the SCN moiety at *ca.* 2133 cm^{-1} (sharp) and 2093 cm^{-1} (broad), indicating the presence of the two isomers in solution. The complex with the thiocyanate group bound by the sulfur atom (the S-isomer) produces an intense and sharp band at *ca.* 2133 cm^{-1} which corresponds to the stretching of the CN bond of the thiocyanate ligand. This band is much broader in the N-isomer and appears at *ca.* 2093 cm^{-1}. The proportion of the two isomers in the solid state, in the mesophase and in CH_2Cl_2 solution has been calculated assuming that the integrated absorption intensity of the ν_{CN} (isothiocyanato) band of an N-isomer is generally about one order of magnitude larger than that of an S-isomer,[20] and the results are collected in Table 1.

It is found that the proportion of the N-isomer present in dichloromethane solution is about 10–15% in each case. Gold(I) is a soft metal and it should prefer to bind the thiocyanate ligand by the soft sulfur atom. However, if the neutral ligand *trans* to the thiocyanate is a strong π acceptor, then the Au–S bond can be weakened enough to make the Au-

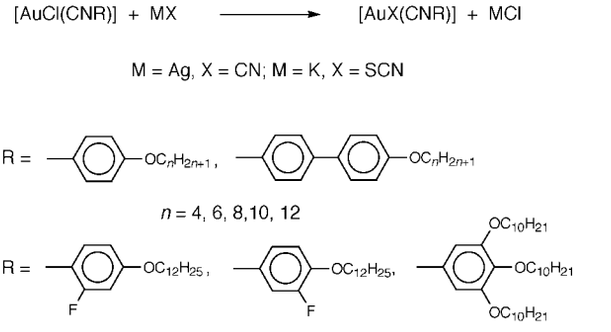

Scheme 1

Table 1 Percentage of S-bonded isomer in selected complexes [Au(thiocyanate)(CNR)] in dichloromethane solution, in the mesophase and in the solid state

R	CH_2Cl_2	Mesophase	Solid
$C_6H_4C_6H_4OC_{12}H_{25}$	90	81	<5
$C_6H_4OC_{12}H_{25}$	90	82	95
2-F-4-$OC_{12}H_{25}C_6H_3$	90	79	73
3-F-4-$OC_{12}H_{25}C_6H_3$	85	86	100
3,4,5-$(OC_{10}H_{21})_3C_6H_2$	91	82	85

SCN and Au-NCS isomers of similar stability, and a mixture of both isomers is isolated. Thus, in complexes where the *trans* ligand is a phosphine, the AuNCS/AuSCN ratio increases as the *trans* influence of the phosphine ligand increases.[20,22,23] Since isocyanides are strong π-acceptors, the presence of some N-isomer should be expected in their gold(I) complexes with thiocyanate. The small differences in *trans*-influence of the diverse isocyanides used did not produce any noticeable effect and the proportion of the N-isomer present in dichloromethane solution was similar in all cases.

It is remarkable that for the biphenyl derivatives the S-bonded isomer is a minor or non-existent component in the solid state. Several factors may influence the Au-NCS/Au-SCN ratio. Thus, it has already been described by us that in the complexes $[AuX(CNC_6H_4C_6H_4OC_nH_{2n+1})]$ (X = halogen),[10] the torsion angle of two aryl rings in the biphenyl group is at a minimum in the solid state and its average value increases as the material melts and its viscosity decreases, making rotation around the C–C single bonds easier. Since the conjugation between the two aryl rings in the biphenyl system is maximum for the minimum torsion angle, the *trans* influence of the biphenylisocyanide ligand must be at a maximum in the solid state and will decrease as the temperature is increased. Thus, the ratio AuNCS/AuSCN for biphenylisocyanide complexes should increase in the solid state, as observed. Nevertheless, packing effects in the solid state may also account for the increased amount of N-isomer observed.

The ^{1}H NMR spectra of the compounds are all similar for each family. At 300 MHz the aromatic hydrogens from *p*-alkoxyphenylisocyanide complexes (which strictly are an AA′BB′ system) show two somewhat distorted 'doublets' in the range 6.9–7.5 ppm, with apparent coupling constants ($N = J_{AB} + J_{AX'}$) of 9.0 Hz. In addition, the first methylene group of the alkoxy chain is observed as a virtual triplet at 3.9–4.1 ppm. The remaining chain hydrogens appear in the range 0.8–1.8 ppm. Analogously, the ^{1}H NMR spectra of biphenylisocyanide complexes show four 'doublets' from aromatic hydrogens (two AA′BB′ spin systems) as reported for similar halocomplexes $[AuX(CNC_6H_4C_6H_4OC_nH_{2n+1})]$ (X = halogen).[10] Independent signals for the two linkage isomers are not observed. Either they overlap or there is a fast exchange between them. The $^{13}C\{^1H\}$ NMR spectrum of the complex $[Au(SCN)(CNC_6H_4C_6H_4OC_{10}H_{21})]$ shows eight singlets at 159.9, 144.8, 130.4, 128.2, 127.8, 127.3, 121.7 and 115.1 ppm from two aromatic rings. Moreover the first methylene group of the alkoxy chain is observed as a singlet at 68.1 ppm, and the remaining chain carbons appear in the range 31.8–14.0 ppm. Again independent signals for the two linkage isomers are not observed in spite of the greater chemical shift differences expected in ^{13}C spectroscopy. Attempts at recording the NMR spectra at low temperature failed due to precipitation of the compounds.

The ^{1}H NMR spectra of the complexes containing fluorinated isocyanides show the corresponding pattern of the AMN part of an AMNX spin system in the range δ 7.0–7.35. The hydrogens of the aliphatic chains appear at similar chemical shifts as for the complexes with non-fluorinated isocyanides. On the other hand, when the isocyanide coordinated to gold(I) bears three alkoxy chains at the 3, 4, and 5 positions of the phenyl ring, the ^{1}H NMR spectrum shows a singlet corresponding to two equivalent aromatic protons at *ca.* δ 7, plus signals for the aliphatic chains. The ^{19}F NMR spectra of the fluorinated complexes show a multiplet (ddd) by coupling of the fluorine atom to the three hydrogens in the ring.

Mesogenic behaviour

The thermal behaviour of the cyano and thiocyanato gold(I) isocyanide complexes prepared is summarized in Table 2 and Fig. 1. None of the phenylisocyanides used in this work are liquid crystals, but most of the complexes are (only the thiocyanate complex with 4-butoxyphenylisocyanide lacks mesogenic character). They display a smectic A (S_A) mesophase showing the typical mielinic and homeotropic textures which reorganize to the fan-shaped texture at temperatures close to the clearing point, and the focal-conic texture on cooling from the isotropic liquid.

The complexes described here have essentially linear geometry, as found by X-ray diffraction for $[Au(CN)(CNCH_3)]$ and other halogold(I) isocyanide complexes.[15,16,24] The simplest way to look at the whole series [AuX(CNR)] (X = CN, SCN; R = $C_6H_4OC_nH_{2n+1}$, 2-F-4-$OC_{12}H_{25}C_6H_3$, 3-F-4-$OC_{12}H_{25}C_6H_3$, $C_6H_4C_6H_4OC_nH_{2n+1}$) is to consider them as formal derivatives of $[AuX(CNC_6H_4OC_nH_{2n+1})]$ (X = CN, SCN) by introduction of a lateral substituent on the phenyl ring (fluorination at the 2- and 3-positions), or addition of a second aromatic ring (biphenyl compounds).

In general, lateral fluorination causes a broadening of the molecule, reducing the intermolecular attractions and leading to lower transition temperatures. On the other hand, polarization effects can cause increased intermolecular interactions, leading to higher transition temperatures. The 2- and 3-fluorinated derivatives differ from each other mainly in their polarization effects, because the position of the fluorine atom does not affect significantly the breadth of the molecule. An electronegative substituent (F) *ortho* to the OR group (3-fluorination) will produce a larger polarization effect than when it is placed in the *meta* position (2-fluorination).[12] Thus, lower intermolecular interactions should be expected in 2-F derivatives, which behave as monotropic. Consequently the transition temperatures should decrease in the order 3-F > 2-F, as observed.

The incorporation of a second phenyl ring in the system (biphenylisocyanide complexes) produces a small increase of the liquid crystal range, possibly due to the greater molecular polarizability of the biphenyl group compared to the phenyl. These complexes melt at temperatures between 86 and 152 °C into a smectic A phase. The free biphenylisocyanides are mesomorphic showing nematic and S_A phases in the range 40–85 °C.

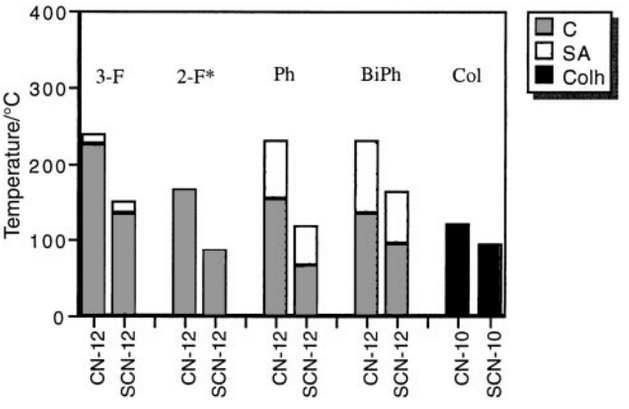

Fig. 1 Thermal behavior of the complexes. The bars are labeled X-*n*; X stands for the pseudohalide, and *n* for the number of carbon atoms in the alkoxy chain. *Monotropic behaviour.

Table 2 Optical, thermal, and thermodynamic data of complexes [AuX(CN-R-OC_nH_{2n+1})] and [AuX{CN-R-(3,4,5-$OC_{10}H_{21})_3$}]

X	R	n	Transition[a]	Temperature[b]/°C	ΔH^b/kJ mol^{-1}
CN	C_6H_4	4	C–S_A	145.0	9.1
			S_A–I	200 (decomp.)[c]	
CN	C_6H_4	6	C–S_A	149.9	8.7
			S_A–I	230 (decomp.)[c]	
CN	C_6H_4	8	C–S_A	159.3	11.7
			S_A–I	230 (decomp.)[c]	
CN	C_6H_4	10	C–S_A	155.8	11.6
			S_A–I	230 (decomp.)[c]	
CN	C_6H_4	12	C–S_A	153.9	12.2
			S_A–I	230 (decomp.)[c]	
SCN	C_6H_4	4	C–I	79.2	15.8
SCN	C_6H_4	6	C–S_A	52.8	19.2
			S_A–I	72.9	2.6
SCN	C_6H_4	8	C–S_A	49.6	9.3
			S_A–I	97.8	3.2
SCN	C_6H_4	10	C–S_A	63.8	30.2
			S_A–I	112.8	3.5
SCN	C_6H_4	12	C–S_A	66.6	37.7
			S_A–I	119.7	3.4
CN	$C_6H_4C_6H_4$	4	C–S_A	152.5	19.3
			S_A–I	210 (decomp.)[c]	
CN	$C_6H_4C_6H_4$	6	C–S_A	151.9	24.7
			S_A–I	225 (decomp.)[c]	
CN	$C_6H_4C_6H_4$	8	C–C′	70.80	7.4
			C′–S_A	144.4	25.47
			S_A–I	225 (decomp.)[c]	
CN	$C_6H_4C_6H_4$	10	C–C′	93.9	7
			C′–S_A	134.2	35.7
			S_A–I	230 (decomp.)[c]	
CN	$C_6H_4C_6H_4$	12	C–S_A	122.7	40.8
			S_A–I	220 (decomp.)[c]	
SCN	$C_6H_4C_6H_4$	4	C–C′	115.2	1.3
			C′–S_A	123.7	50.8
			S_A–I	178 (decomp.)[c]	
SCN	$C_6H_4C_6H_4$	6	C–S_A	109.1	59.2
			S_A–I	168 (decomp.)[c]	
SCN	$C_6H_4C_6H_4$	8	C–S_A	86.1	52.3
			S_A–I	145 (decomp.)[c]	
SCN	$C_6H_4C_6H_4$	10	C–S_A	97.0	67.1
			S_A–I	140 (decomp.)[c]	
SCN	$C_6H_4C_6H_4$	12	C–S_A	94.2	55.6
			S_A–I	164 (decomp.)[c]	
CN	2-FC_6H_3	12	C–C′	123.7	19.8
			C–I	166.0	34.1
			I–S_A+C	103.4	−14.9
SCN	2-FC_6H_3	12	C–C′	76.4	1.4
			C–I	86.2	48.6
			I–S_A	65.4	−3.1
			S_A–C	56.3	−32.5
CN	3-FC_6H_3	12	C–C′	100.6	3.8
			C′–C″	120.6	3.8
			C″–C‴	129.1	4.2
			C‴–S_A	225 (decomp.)[c]	19.7
SCN	3-FC_6H_3	12	C–C′	73.1	19.5
			C′–C″	84.4	9.6
			C–S_A	136.3	27.9
			S_A–I	149.0	3.4
CN	C_6H_2	10	D_h–I	121.1	2.6
SCN	C_6H_2	10	D_h–I	94.6	2.5

[a]C, crystal; S, smectic; I, isotropic liquid. [b]Data refer to the second DSC cycle, starting from a temperature close to the melting point. Temperature data as peak onset. [c]Data from the microscope.

The introduction of two additional alkoxy chains in the phenyl group (3,4,5-trialkoxyphenyl complexes) causes a dramatic change in the structure of the molecule, which cannot be considered rod-like any longer. Consistently, the complexes show hexagonal columnar mesophases at room temperature. Their crystallization is not observed due to supercooling of the mesophase. The optical textures, when viewed with a polarizing microscope on cooling from the isotropic liquid, are characteristic of hexagonal columnar mesophases and display linear birefringent defects, large areas of uniform extinction and fan domains.

X-Ray diffraction studies performed on the mesophase of complex [Au(SCN){CNC_6H_4-3,4,5-($OC_{10}H_{21})_3$}] reveal five low-angle rings, a diffuse ring at an intermediate angle, and two broad rings at high angles (Fig. 2). The diameters of the reflections at low angles are in the ratio $1:3^{1/2}:4^{1/2}:7^{1/2}:9^{1/2}$ indicating that the molecules are ordered in a two-dimensional hexagonal lattice with $a=30.8$ Å. The broad ring at 4.4 Å shows that the alkyl chains have a liquid-like structure, while the other at 3.3 Å indicates that the aromatic cores are stacked together to form columns. Thus, the mesophase is hexagonal columnar. These data are consistent with a disc formed by two

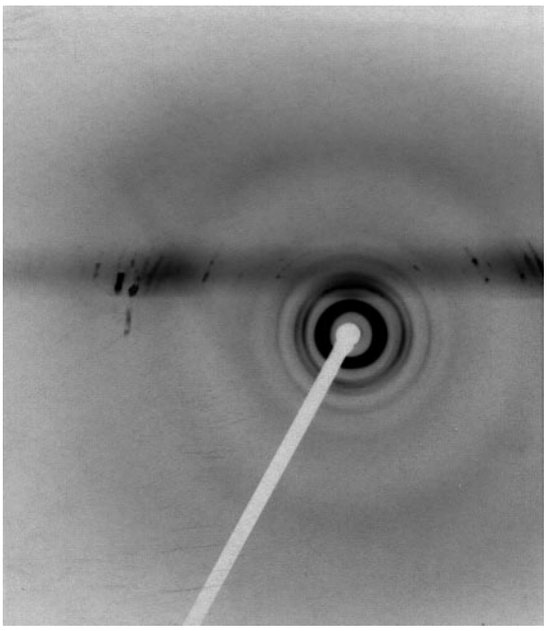

Fig. 2 X-Ray diffraction pattern for [Au(SCN){C≡NC$_6$H$_2$-3,4,5-(OC$_{10}$H$_{21}$)$_3$}] at ambient temperature.

molecules of the complex in antiparallel disposition, similar to that reported for the analogous chlorogold complexes.[11]

The presence of the broad band at 3.3 Å in the X-ray pattern of the SCN complexes is indicative of a higher order inside the columns in comparison with the chloro complexes, but its diffuse nature shows that the coherence length is not very high. The presence of the diffuse ring at an intermediate angle is not easy to explain, therefore another X-ray diffraction experiment was performed from the mesophase mechanically oriented over a mica sheet (Fig. 3). The new X-ray pattern displayed two diffuse spots at 6.5 Å in the equatorial plane, corresponding to the diffuse ring in the former experiment. Thus, their origin is the interference between the two gold atoms in each disc. The existence of the diffuse ring at 6.5 Å and the outer ring at 3.3 Å suggests higher intermolecular interactions in the SCN complex than in the chloro complex (these reflections are not seen in the chloro complex).[11] This is in agreement with the observed trend in the clearing points (SCN > Cl).

Some derivatives show some decomposition at, or just above, the clearing point, possibly due to their high transition temperatures. The increase of the length of the chain in the cyano alkoxyphenyl and biphenylisocyanide derivatives does not produce significant variation in their transition temperatures. However, in the thiocyanate complexes with alkoxyphenylisocyanides the melting points clearly decrease as the length of the alkoxy chain increases, to reach a minimum for $n = 8$ and beyond, whereas the clearing temperatures increase moderately with the length of the chain. As a consequence of these two trends the range of mesogenic behaviour for SCN complexes increases for long chains. The moderate increase in the clearing temperatures can be associated with an increase in the contribution to the polarizability of the molecule by the longer chains.

Irrespective of the isocyanide used, the variation in transition temperatures is quite regular, decreasing in the order CN > SCN. This can be explained by taking into account that the thiocyanate derivatives are actually a mixture of two isomers, while the cyano complexes are pure compounds. On the other hand, it is apparent from the space-filling models of the cyano- and thiocyanato-gold complexes shown in Fig. 4 that the total length of the molecule is not affected on going from CN to SCN, but a clear increase in the molecular breadth (considering the molecule as a cylinder) is produced.[25] Therefore lower transition temperatures are expected for the wider molecules, as observed.

Finally, the existence of two isomers in both the solid state and the mesophase of the thiocyanate derivatives and the displacement of the equilibrium between them in the melting process (Table 1) preclude comparisons with the halogold isocyanide complexes. However, the cyano derivatives have a larger dipole moment than the halogold complexes and, consequently, display higher transition points.

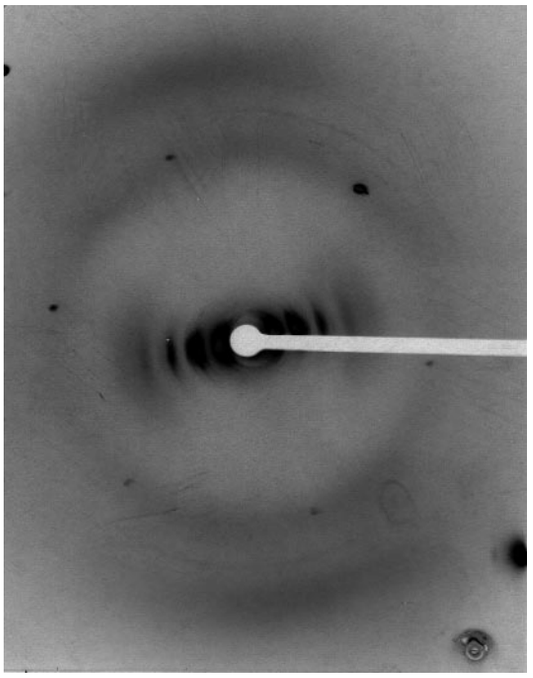

Fig. 3 X-Ray diffraction pattern for [Au(SCN){C≡NC$_6$H$_2$-3,4,5-(OC$_{10}$H$_{21}$)$_3$}] at ambient temperature of a sample mechanically oriented over a mica sheet.

Experimental

Materials and techniques

Combustion analyses were made with a Perkin-Elmer 2400 microanalyzer. IR spectra were recorded on a Perkin-Elmer FT 1720X instrument. The ratios of the *ν*(CN) integrated absorption intensities of N-bonded/S-bonded thiocyanates were calculated as reported.[20] IR spectra of samples in the mesophase were recorded between thin plates (about 0.5 mm) of NaCl using a Mettler FP82HT hot stage without the glass

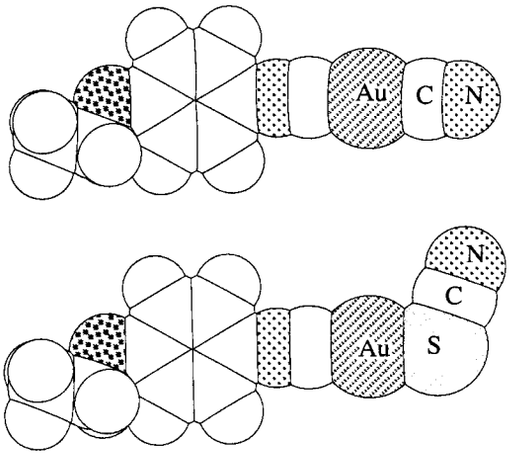

Fig. 4 Space-filling model of the complexes [AuX(C≡NC$_6$H$_4$O-C$_2$H$_5$-*p*)] (X = CN, SCN) showing the shape and size variation introduced by the change of pseudohalide.

heat shield and a Mettler FP90 central processor.[26] ^{1}H and $^{13}C\{^{1}H\}$ NMR spectra were recorded using a Bruker AC-300 instrument (solvent $CDCl_3$). Microscopy studies were carried out using a Leitz microscope, equipped with a hot stage and polarizers, at a heating rate of *ca.* 10 °C min^{-1}. For differential scanning calorimetry (DSC) a Perkin-Elmer DSC7 instrument was used, which was calibrated with water and indium; the scanning rate was 10 °C min^{-1}, the samples were sealed in aluminium capsules in the air, and the holder atmosphere was dry nitrogen.

[AuCl(CNR)] (R = $C_6H_4OC_nH_{2n+1}$-*p*, $C_6H_4C_6H_4OC_nH_{2n+1}$-*p*, C_6H_3(2-F)$OC_{12}H_{25}$, C_6H_2(3,4,5-$OC_{12}H_{25}$)$_3$) were prepared by literature methods.[8,10,11]

Preparation of the compounds

All compounds [AuX(CNR)] (X = CN, SCN) were prepared similarly from the corresponding [AuCl(CNR)] complexes by exchange reaction with AgCN and KSCN salts respectively. Only representative examples are described as the syntheses were similar for the rest of the complexes.

Preparation of [Au(CN){C≡N(C_6H_4)$_m$$OC_nH_{2n+1}$-*p*}]. Solid wet AgCN, freshly prepared from $AgNO_3$ (0.150 g, 0.930 mmol) and KCN (0.060 g, 0.930 mmol) in water, was added to [AuCl{C≡N(C_6H_4)$_m$$OC_nH_{2n+1}$-*p*}] (0.190 mmol) dissolved in dichloromethane (30 mL). The mixture was stirred for 30 min and then dried over anhydrous magnesium sulfate and filtered. The solvent was reduced to 10 mL under reduced pressure and ethanol (10 mL) was added to obtain white crystals of the product.

m = 1: *n* = 4: Yield 40%. IR *ν*(C≡N)/cm^{-1}: (CH_2Cl_2) 2229 (CNR), 2159 (CN); (Nujol) 2244, 2232 (CNR), 2159 (CN). Anal. Calc. for $C_{12}H_{13}AuN_2O$: C, 36.20; H, 3.29; N, 7.04. Found: C, 35.84; H, 3.19; N, 6.63%. *n* = 6: Yield 40%. IR *ν*(C≡N)/cm^{-1}: (CH_2Cl_2) 2229 (CNR), 2159 (CN); (Nujol) 2246, 2228 (CNR), 2159 (CN). Anal. Calc. for $C_{14}H_{17}AuN_2O$: C, 39.45; H, 4.02; N, 6.57. Found: C, 38.88; H, 3.81; N, 6.58%. *n* = 8: Yield 66%. IR *ν*(C≡N)/cm^{-1}: (CH_2Cl_2) 2229 (CNR), 2159 (CN); (Nujol) 2241, 2216 (CNR), 2158 (CN). Anal. Calc. for $C_{16}H_{21}AuN_2O$: C, 42.30; H, 4.66; N, 6.17. Found: C, 42.13; H, 4.38; N, 6.03%. *n* = 10: Yield 62%. IR *ν*(C≡N)/cm^{-1}: (CH_2Cl_2) 2229 (CNR), 2159 (CN); (Nujol) 2244, 2217 (CNR), 2158 (CN). Anal. Calc. for $C_{18}H_{25}AuN_2O$: C, 44.82; H, 5.22; N, 5.81. Found: C, 44.91; H, 5.01; N, 5.67%. *n* = 12: Yield 64%. IR *ν*(C≡N)/cm^{-1}: (CH_2Cl_2) 2229 (CNR), 2159 (CN); (Nujol) 2243, 2217 (CNR), 2158 (CN). Anal. Calc. for $C_{20}H_{29}AuN_2O$: C, 47.06; H, 5.73; N, 5.49. Found: C, 46.40; H, 5.32; N, 5.27%.

m = 2: *n* = 4: Yield 52%. IR *ν*(C≡N)/cm^{-1}: (CH_2Cl_2) 2230 (CNR), 2160 (CN); (Nujol) 2249 (CNR), 2160 (CN). Anal. Calc. for $C_{18}H_{17}AuN_2O$: C, 45.58; H, 3.61; N, 5.91. Found: C, 44.99; H, 3.56; N, 5.81%. *n* = 6: Yield 50%. IR *ν*(C≡N)/cm^{-1}: (CH_2Cl_2) 2230 (CNR), 2160 (CN); (Nujol) 2250 (CNR), 2158 (CN). Anal. Calc. for $C_{20}H_{21}AuN_2O$: C, 47.83; H, 4.21; N, 5.58. Found: C, 48.02; H, 4.12; N, 5.31%. *n* = 8: Yield 46%. IR *ν*(C≡N)/cm^{-1}: (CH_2Cl_2) 2230 (CNR), 2160 (CN); (Nujol) 2250 (CNR), 2158 (CN). Anal. Calc. for $C_{22}H_{25}AuN_2O$: C, 49.82; H, 4.75; N, 5.28. Found: C, 50.02; H, 4.71; N, 5.32%. *n* = 10: Yield 53%. IR *ν*(C≡N)/cm^{-1}: (CH_2Cl_2) 2230 (CNR), 2159 (CN); (Nujol) 2250 (CNR), 2158 (CN). Anal. Calc. for $C_{24}H_{29}AuN_2O$: C, 51.62; H, 5.23; N, 5.02. Found: C, 52.05; H, 5.15; N, 4.84%. *n* = 12: Yield 41%. IR *ν*(C≡N)/cm^{-1}: (CH_2Cl_2) 2230 (CNR), 2159 (CN); (Nujol) 2250 (CNR), 2158 (CN). Anal. Calc. for $C_{26}H_{33}AuN_2O$: C, 53.24; H, 5.67; N, 4.78. Found: C, 53.57; H, 5.65; N, 4.32%.

Preparation of [Au(SCN){C≡N(C_6H_4)$_m$$OC_nH_{2n+1}$-*p*}]. The method followed was the same as above but using KSCN (0.036 g, 0.370 mmol) instead of AgCN.

m = 1: *n* = 4: Yield 58%. IR *ν*(C≡N)/cm^{-1}: (CH_2Cl_2) 2224 (CNR), 2133, 2095 (SCN); (Nujol) 2230 (CNR), 2103 (SCN). Anal. Calc. for $C_{12}H_{13}AuN_2OS$: C, 33.50; H, 3.05; N, 6.51. Found: C, 33.49; H, 3.17; N, 6.55%. *n* = 6: Yield 59%. IR *ν*(C≡N)/cm^{-1}: (CH_2Cl_2) 2224 (CNR), 2133, 2092 (SCN); (Nujol) 2228 (CNR), 2131 (SCN). Anal. Calc. for $C_{14}H_{17}AuN_2OS$: C, 36.69; H, 3.74; N, 6.11. Found: C, 36.67; H, 3.77; N, 6.24%. *n* = 8: Yield 48%. IR *ν*(C≡N)/cm^{-1}: (CH_2Cl_2) 2224 (CNR), 2133, 2091 (SCN); (Nujol) 2228 (CNR), 2131 (SCN). Anal. Calc. for $C_{16}H_{21}AuN_2OS$: C, 39.51; H, 4.35; N, 5.76. Found: C, 39.35; H, 4.26; N, 6.04%. *n* = 10: Yield 68%. IR *ν*(C≡N)/cm^{-1}: (CH_2Cl_2) 2224 (CNR), 2133, 2092 (SCN); (Nujol) 2223 (CNR), 2134, 2125 (SCN). Anal. Calc. for $C_{18}H_{25}AuN_2OS$: C, 42.03; H, 4.90; N, 5.45. Found: C, 42.02; H, 4.90; N, 5.42%. *n* = 12: Yield 76%. IR *ν*(C≡N)/cm^{-1}: (CH_2Cl_2) 2224 (CNR), 2133, 2092 (SCN); (Nujol) 2222 (CNR), 2134, 2125 (SCN). Anal. Calc. for $C_{20}H_{29}AuN_2OS$: C, 44.28; H, 5.39; N, 5.16. Found: C, 44.74; H, 5.39; N, 5.06%.

m = 2: *n* = 4: Yield 91%. IR *ν*(C≡N)/cm^{-1}: (CH_2Cl_2): 2225 (CNR), 2134, 2093 (SCN); (Nujol): 2228 (CNR), 2085 (SCN). Anal. Calc. for $C_{18}H_{17}AuN_2OS$: C, 42.69; H, 3.38; N, 5.53. Found: C, 42.65; H, 3.38; N, 5.57%. *n* = 6: Yield 81%. IR *ν*(C≡N)/cm^{-1}: (CH_2Cl_2) 2225 (CNR), 2134, 2093 (SCN); (Nujol) 2227 (CNR), 2086 (SCN). Anal. Calc. for $C_{20}H_{21}AuN_2OS$: C, 44.95; H, 3.96; N, 5.24. Found: C, 44.80; H, 3.70; N, 5.25%. *n* = 8: Yield 95%. IR *ν*(C≡N)/cm^{-1}: (CH_2Cl_2) 2225 (CNR), 2134, 2093 (SCN); (Nujol) 2230 (CNR), 2099 (SCN). Anal. Calc. for $C_{22}H_{25}AuN_2OS$: C, 46.98; H, 4.48; N, 4.98. Found: C, 46.76; H, 4.26; N, 4.96%. *n* = 10: Yield 69%. IR *ν*(C≡N)/cm^{-1}: (CH_2Cl_2) 2224 (CNR), 2134, 2092 (SCN); (Nujol) 2228 (CNR), 2086 (SCN). Anal. Calc. for $C_{24}H_{29}AuN_2OS$: C, 48.81; H, 4.95; N, 4.74. Found: C, 48.58; H, 4.68; N, 4.82%. *n* = 12: Yield 81%. IR *ν*(C≡N)/cm^{-1}: (CH_2Cl_2) 2224 (CNR), 2134, 2093 (SCN); (Nujol) 2232 (CNR), 2087 (SCN). Anal. Calc. for $C_{26}H_{33}AuN_2OS$: C, 50.48; H, 5.38; N, 4.53. Found: C, 50.89; H, 5.06; N, 4.95%.

[AuX(CNR)]: R = 2-F-4-$OC_{12}H_{25}C_6H_3$. X = CN: Yield 63%. IR *ν*(C≡N)/cm^{-1}: (CH_2Cl_2) 2229 (CNR), 2134, 2093 (SCN); (Nujol) 2239 (CNR), 2158 (SCN). Anal. Calc. for $C_{26}H_{29}AuN_2OS$: C, 45.46; H, 5.34; N, 5.30. Found: C, 45.59; H, 5.15; N, 5.25%. X = SCN: Yield 56%. IR *ν*(C≡N)/cm^{-1}: (CH_2Cl_2) 2223 (CNR), 2134, 2093 (SCN); (Nujol) 2236 (CNR), 2132 (SCN). Anal. Calc. for $C_{26}H_{29}AuN_2OS$: C, 42.86; H, 5.04; N, 5.00. Found: C, 42.99; H, 4.82; N, 4.63%.

R = 3-F-4-$OC_{12}H_{25}C_6H_3$. X = CN: Yield 62%. IR *ν*(C≡N)/cm^{-1}: (CH_2Cl_2) 2229 (CNR), 2134, 2093 (SCN); (Nujol) 2252 (CNR), 2168 (SCN). Anal. Calc. for $C_{26}H_{29}AuN_2OS$: C, 45.46; H, 5.34; N, 5.30. Found: C, 45.42; H, 5.27; N, 5.29%. X = SCN: Yield 72%. IR *ν*(C≡N)/cm^{-1}: (CH_2Cl_2) 2218 (CNR), 2133, 2129 (SCN); (Nujol) 2233 (CNR), 2129 (SCN). Anal. Calc. for $C_{26}H_{29}AuN_2OS$: C, 42.86; H, 5.04; N, 5.00. Found: C, 43.01; H, 4.95; N, 4.79%.

R = 3,4,5-($OC_{10}H_{21}$)$_3$$C_6H_2$. X = CN: Yield 62%. IR *ν*(C≡N)/cm^{-1}: (CH_2Cl_2) 2227 (CNR), 2160 (CN); (Nujol) 2230 (CNR), 2144 (CN). Anal. Calc. for $C_{38}H_{65}AuN_2O_3$: C, 57.42; H, 8.24; N, 3.52. Found: C, 57.89; H, 8.09; N, 3.39%. X = SCN: Yield 72%. IR *ν*(C≡N)/cm^{-1}: (CH_2Cl_2) 2225 (CNR), 2133, 2090 (SCN); (Nujol) 2226 (CNR), 2124, 2088 (SCN). Anal. Calc. for $C_{38}H_{65}AuN_2O_3S$: C, 55.19; H, 7.92; N, 3.39. Found: C, 55.60; H, 7.87; N, 3.21%.

Acknowledgements

We are indebted to the Comisión Interministerial de Ciencia y Tecnología (Project MAT96-0708) and to the Junta de Castilla y León (Project VA23/97) for financial support. We are

indebted to Dr. Anne-Marie Levelut for the use of the Guinier camera and helpful discussions.

References

1 A. M. Giroud-Godquin and P. M. Maitlis, *Angew. Chem., Int. Ed. Engl.*, 1991, **30**, 375.
2 P. Espinet, M. A. Esteruelas, L. A. Oro, J. L. Serrano and E. Sola, *Coord. Chem. Rev.*, 1992, **117**, 215.
3 *Inorganic Materials*, ed. D. W. Bruce and D. O'Hare, John Wiley & Sons, Chichester, 1992, ch. 8.
4 S. A. Hudson and P. M. Maitlis, *Chem. Rev.*, 1993, **93**, 861.
5 *Metallomesogens*, ed. J. L. Serrano, VCH, Weinheim, 1996.
6 T. Kaharu, T. Tanaka, M. Sawada and S. Takahashi, *J. Mater. Chem.*, 1994, **4**, 859.
7 R. Ishii, T. Kaharu, N. Pirio, S.-W. Zhang and S. Takahashi, *J. Chem. Soc., Chem. Commun.*, 1995, 1215.
8 S. Coco, P. Espinet, S. Falagán and J. M. Martín-Alvarez, *New J. Chem.*, 1995, **19**, 959.
9 P. Alejos, S. Coco and P. Espinet, *New J. Chem.*, 1995, **19**, 799.
10 M. Benouazzane, S. Coco, P. Espinet and J. M. Martín-Alvarez, *J. Mater. Chem.*, 1995, **5**, 441.
11 S. Coco, P. Espinet, J. M. Martín-Alvarez and A. M. Levelut, *J. Mater. Chem.*, 1997, **7**, 19.
12 R. Bayón, S. Coco, P. Espinet, C. Fernández-Mayordomo and J. M. Martín-Alvarez, *Inorg. Chem.*, 1997, **36**, 2329.
13 H. Adams, N. A. Bailey, D. W. Bruce, R. Dhillon, D. Dummur, S. E. Hunt, E. Lalinde, A. A. Maggs, R. Orr, P. Stiring, M. S. Wragg and P. M. Maitlis, *Polyhedron*, 1988, **7**, 1861.
14 M. M. El-Etri and W. M. Scovell, *Inorg. Chem.*, 1990, **29**, 480.
15 C.-M. Che, H.-K. Yip, W.-T. Wong and T.-F. Lai, *Inorg. Chim. Acta*, 1992, **197**, 177.
16 S. Esperas, *Acta Chem. Scand. A*, 1976, **30**, 527.
17 K. Nakamoto, *Infrared Spectra of Inorganic and Coordination Compounds*, John Wiley & Sons, New York, 1970.
18 N. J. Destefano and J. L. Burmeister, *Inorg. Chem.*, 1971, **10**, 998.
19 J. L. Burmeister and J. B. Melpolder, *J. Chem. Soc. Chem. Commun.*, 1973, 613.
20 J. B. Melpolder and J. L. Burmeister, *Inorg. Chim. Acta*, 1981, **49**, 115.
21 A. H. Norbury, *Adv. Inorg. Chem. Radiochem.*, 1975, **17**, 232.
22 J. L. Burmeister and F. Basolo, *Inorg. Chem.*, 1964, **3**, 1587.
23 N. N. Akhtar, A. A. Isab, A. R. Al-Arfaj and M. S. Hussain, *Polyhedron*, 1997, **16**, 125.
24 W. Schneider, K. Angermaier, A. Sladek and H. Schmidbaur, *Z. Naturforsch., Teil B*, 1996, **51**, 790.
25 This is true for the major Au-SCN isomer, which is the one represented in Fig. 4; the minor Au-NCS isomer should probably be linear, acording to literature data (ref. 20).
26 S. Coco, F. Díez-Expósito, P. Espinet, C. Férnandez-Mayordomo, J. M. Martín-Alvarez and A. M. Levelut, *Chem. Mater.*, 1998, **10**, 3666.

Paper 9/04078A